Bacterial swimmers that infiltrate and take over the biofilm matrix

Ali Houry[a,b], Michel Gohar[a,b], Julien Deschamps[a,b], Ekaterina Tischenko[a,b], Stéphane Aymerich[a,b], Alexandra Gruss[a,b], and Romain Briandet[a,b,1]

[a]INRA (Institut National de la Recherche Agronomique), Micalis Institute (UMR1319), F-78350 Jouy-en-Josas, France; and [b]AgroParisTech, Micalis Institute (UMR), F-78350 Jouy-en-Josas, France

Bacteria grow in either planktonic form or as biofilms, which are attached to either inert or biological surfaces. Both growth forms are highly relevant states in nature and of paramount scientific focus. However, interchanges between bacteria in these two states have been little explored. We discovered that a subpopulation of planktonic bacilli is propelled by flagella to tunnel deep within a biofilm structure. Swimmers create transient pores that increase macromolecular transfer within the biofilm. Irrigation of the biofilm by swimmer bacteria may improve biofilm bacterial fitness by increasing nutrient flow in the matrix. However, we show that the opposite may also occur (i.e., swimmers can exacerbate killing of biofilm bacteria by facilitating penetration of toxic substances from the environment). We combined these observations with the fact that numerous bacteria produce antimicrobial substances in nature. We hypothesized and proved that motile bacilli expressing a bactericide can also kill a heterologous biofilm population, *Staphylococcus aureus* in this case, and then occupy the newly created space. These findings identify microbial motility as a determinant of the biofilm landscape and add motility to the complement of traits contributing to rapid alterations in biofilm populations.

bacterial ecology | biofilm disruption | motile subpopulations | antimicrobials | time-lapse confocal imaging

Microbial biofilms constitute the major lifestyle alternative to planktonic growth and are commonly formed on inert or living surfaces. In these biological structures, cells are held together in a 3D organization by self-produced extracellular polymeric substances (EPSs). EPS composition varies greatly depending on the biofilm ecosystem but typically contains a mixture of principally polysaccharides, as well as proteins, nucleic acids, and lipids (1). This complex mixture of hydrated biomolecules is responsible for matrix strength and biofilm viscoelastic properties by means of weak physicochemical interactions (e.g., van der Waals, Lewis acid–base, and electrostatic interactions; polymers; entanglement involving flagella or pili) (1). The development of this spatial organization results in molecular gradients within the matrix of nutrients, oxygen, and signaling molecules, which generate local physiological and genetic heterogeneities (2). The matrix can also act as a "protective shield" against the diffusion and action of antimicrobials in the bulk of the biofilm (3), thus posing a serious problem for treatment of biofilm-related infections and for microbial elimination in industrial settings (4). According to National Institutes of Health estimates, biofilms account for over 80% of human microbial infections (http://grants.nih.gov/grants/guide/pa-files/PA-03-047.html).

Biofilms are dynamic structures that may be subject to population shifts in response to microbial composition and environmental conditions. Numerous factors of microbial competitiveness (e.g., nutritional fitness, resistance, growth rate) may have an impact on both sessile and planktonic populations (5, 6). Other factors appear to be specific to biofilms (2, 7). Our studies led us to examine the role of motility, studied mainly in planktonic populations to date, on bacterial integrity in biofilms. Bacterial flagella were previously reported to have a positive role in nascent biofilm maturation and spreading (e.g., *Bacillus subtilis*, *Pseudomonas* sp.) (8, 9). However, motile cells in mature biofilms have thus far been described as arising from a late-stage differentiation event (e.g., within hollow voids of *Pseudomonas aeruginosa* mushroom-like structures) and being involved in dispersion of mature biofilms (10).

Here, we report the discovery of highly motile populations within the entire biofilm matrix of several bacilli and other flagellated bacteria in early stage and mature biofilms. These movements generate short-lived pores that irrigate the biofilm and facilitate entry of macromolecules, including antimicrobials. Importantly, we illustrate how planktonic motile bacteria with high kinetic energy, such as motile bacilli, can act as invaders, leading to dissolution of heterologous biofilms and repopulation of the matrix.

Results

Motile Bacteria Generate Pores in the Biofilm Matrix. We examined biofilm formation by the motile bacterium *Bacillus thuringiensis* 407. The majority of cells in the biofilm matrix oscillate in a volume limited to their own cell size (a few micrometers), as expected for constrained sessile bacteria (11). However, time-lapse confocal laser microscopy uncovered the existence of motile subpopulations in the mature biofilm, estimated to represent between 0.1% and 1% of the total population (Fig. 1 and Movie S1). Observed movements are flagella-propelled because they were not detected with flagella-deficient (Δfla) or immobile (ΔmotA) mutants (Movie S2). Bacteria moved up to 16 μm/s in all directions, following different paths through the biofilm mass. Swimming cells passing through the bulk of the biofilm created transient tunnels that lasted for about 2–5 s, highlighting the reversible elastic properties of the matrix (1, 12). In addition to linear movement, rapid circular movements of bacterial chains generated local dispersion and large transient pores (~10 μm diameter), as visible in the still frame from Movie S1 (Fig. 1). Typical chain rotation frequencies were about 0.2 Hz. The tunneling phenomenon was observed in flow cell biofilms as above and also in a microplate batch system (below), suggesting that flow of the liquid medium is not compulsory for this phenomenon.

In a second set of experiments, exponential phase GFP-labeled *B. thuringiensis* cells were deposited onto unlabeled *B. thuringiensis* biofilms. After less than 15 min, fluorescent swimming cells were visualized at the base of the biofilm (Movie S3). The rapidity of this event gives strong evidence that the swimmers detected in biofilms are supplied by the liquid planktonic phase and infiltrate

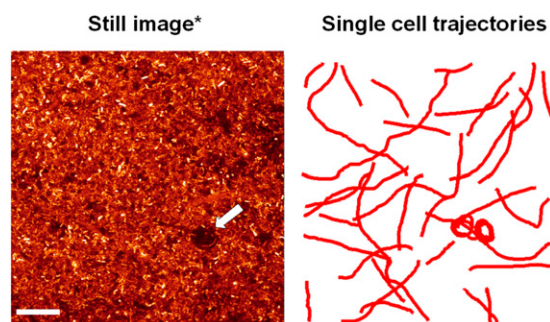**Still image***   **Single cell trajectories**

Fig. 1. *B. thuringiensis* 407 swimmers tunnel into homologous biofilms. Motile bacilli generate pores in the 48-h biofilm matrix. The arrow in the still image indicates a large transient pore formed by the rotation of a motile chain. (Scale bar, 20 μm.) *Taken from Movie S1.

the biofilm matrix. This also excludes the possibility that a mutational event is required for swimming in biofilms. We therefore consider it likely that the swimmers observed in biofilms issue from the planktonic population.

Tests for the capacity of other flagellated bacteria to generate pores within their own biofilm structures indicate that biofilm swimming may be widespread: One of four tested isolates (Table S1) of the Gram-negative motile bacterium *Yersinia enterocolitica* displayed a phenotype similar to that of *B. thuringiensis* 407 (CIP 106676; as shown in Movie S4, kindly provided by M. Naïtali, AgroParisTech). However, strains of motile species *Pseudomonas aeruginosa* (ATCC 1592) and *Bacillus subtilis* (168) did not detectably irrigate their own biofilms in our test conditions. Swimming in such biostructures might require sufficient kinetic energy to overcome the cohesive force generated by the EPS, and would thus vary according to the "swimmer" and the target biofilm (1, 11, 12). It is also possible that biofilm bacteria modulate stealth swimmer activity via signaling molecules that inhibit motility within the matrix.

Impact of Biofilm Age on Tunnel Formation. The properties of tunnels generated in *B. thuringiensis* 407 biofilms were followed as a function of biofilm age. The time courses of biofilm macrostructure and swimmer velocities were recorded over a 3-d period (Fig. S1). The average velocity of swimmer cells, estimated by tracking ~50 single cell trajectories in four microscopic fields, ranged from 7.3 μm/s at 24 h of biofilm growth to 4.2 μm/s at 72 h of biofilm growth. In this dataset, the prevalent proportion of swimmers traveled faster at 24 h (7 μm/s) than at 72 h (about 2 μm/s); at 72 h, short chains adopted a snake-like motion to burrow through the dense network of sessile cells. Thus, although bacterial motility within biofilms progressively slowed with the age of biofilms, a swimming subpopulation remained active within biofilms for at least 72 h.

Changes in viscoelastic properties of the *B. thuringiensis* matrix could account, at least in part, for reduced swimming trajectories in the older biofilms. We observed that sessile cell oscillations, which are inversely correlated with the matrix strength (11), were 25% lower in 72-h biofilms compared with 24-h samples ($P < 0.05$). In the case of *B. thuringiensis* 407, this could be correlated with changes in the matrix exopolysaccharide density, which increased from 17 μg/mm³ at 24 h to 49 μg/mm³ at 72 h ($P < 0.05$).

To determine whether the state of the matrix is responsible for the slower speed of swimmers in older biofilms, we evaluated the behavior of freshly introduced planktonic GFP-labeled *B. thuringiensis* 407 cells in established 24-h-old or 72-h-old nonfluorescent biofilms. Quantification of fluorescence 2 h after depositing the motile fluorescent cells revealed that eightfold more cells integrated in the 24-h biofilm than in the 72-h biofilm (800 vs.

100 μm³ of cells expressing GFP, respectively; $P < 0.05$). These results indicate that biofilm age and matrix viscoelastic properties are important determinants for swimming activity in biofilms.

Penetration of Macromolecules in Biofilms Is Facilitated by Swimmer Bacteria. We hypothesized that pores created by motile bacilli generate microcurrents that facilitate solute access to the deeper biofilm layers. A high-molecular-weight fluorescent macromolecular tracer (FITC–dextran, 250 kDa) was used to mimic the solute. Time-lapse confocal imaging was used to follow its entry in *B. thuringiensis* 407 biofilms comprising motile (*Bt* WT) or nonmotile (*Bt* ΔmotA) bacteria. Note that *Bt* and *Bt* ΔmotA biofilms show similar geometrical metrics (no significant differences in biovolume, thickness, and roughness and permeability to swimmers, as determined by confocal imaging and image analysis) (13). In conditions of shear stress, the motile *Bt* subpopulation in WT biofilms promotes spreading on the biofilm surface, which is not observed in *Bt* ΔmotA biofilms (13); however, this phenomenon does not have an impact on biofilm spatial organization. Migration of FITC–dextran into the basal layer of *Bt* WT and *Bt* ΔmotA was monitored as fluorescence deep within the biofilm structure, at ~5 μm from the inert surface (Fig. 2A). The initial slope value for fluorescence curves (reflecting FITC–dextran migration) from *Bt* ΔmotA biofilms reflects a 1-log lower rate of FITC–dextran penetration compared with the rate using the *Bt* WT swimmer strain (Fig. 2B).

These results show that mechanical movements of motile bacteria contribute to a dynamic environment within biofilm by promoting molecular exchanges between its different layers and with external medium. We suggest that swimmers would thereby facilitate solute exchange and dissipation of harsh local environments generated within biofilms.

Motile Bacilli Penetrate Biofilms Comprising a Heterologous Species. The biofilms generated by bacteria may be markedly different with respect to their viscoelastic properties, relating to differences in their EPS composition. Above a critical kinetic energy specific to each matrix, a motile swimmer can generate a reversible transient elastic response and/or an irreversible deformation (1, 12). We therefore tested the capacity of motile *B. thuringiensis* 407 to tunnel into biofilms comprising different Gram-positive or Gram-negative pathogens (Table S1): *Staphylococcus aureus* RN4220
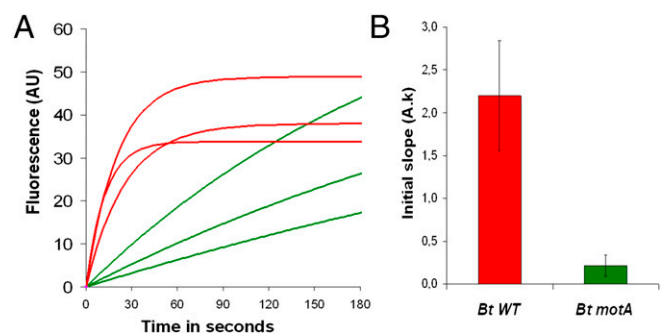

Fig. 2. Penetration of macromolecules in biofilms is facilitated by swimmer bacteria. (A) Penetration of FITC–Dextran in the basal layer of *B. thuringiensis* 407 biofilms comprising the motile WT strain (*Bt* WT in red) or a nonmotile mutant strain (*Bt* ΔmotA in green). Images were captured immediately after FITC–Dextran introduction in the bulk medium. The presented curves are the fits of experimental fluorescence data with the regression model: FI = A.(1 − e^{-kt}), where FI is the fluorescence intensity, A is the maximum fluorescence reached, k is a rate constant, and A.k is the initial slope of the curves. AU, arbitrary unit. (B) Initial slope (A.k) is reduced by one order of magnitude in the absence of tunneling ($P < 0.05$ between *Bt* WT and *Bt* ΔmotA).

Houry et al.

MICROBIOLOGY

(Movie S5), *Enterococcus faecalis* (ATCC 700802; as shown in Movie S6), *Y. enterocolitica* (CIP 81.41), *P. aeruginosa* (ATCC 1592), or *Listeria monocytogenes* (ATCC BAA-679). These selected strains were confirmed to lack the "swimmer phenotype" within their same species biofilms. All these strains were permissive to the heterologous bacillus swimmers.

We tested other swimmers: four *Bacillus licheniformis* isolates, two *B. subtilis* strains, and two *Bacillus cereus* strains (Table S1) were used in experiments with *S. aureus* RN4220 biofilms (shown with *B. licheniformis* LMG 7560 in Movie S7). Four of the eight tested motile bacilli were obtained as isolates from surfaces in medical or industrial equipment (Table S1). Tunneling was observed with all tested motile bacilli, suggesting that stealth swimming in heterologous biofilms is a likely occurrence in natural environments.

We observed that *B. thuringiensis* 407 also infiltrated *B. subtilis* 168 biofilms. Swimming activity was also tested in a biofilm comprising a *B. subtilis* 168 Δ*abrB* mutant, in which matrix components and biofilm formation are up-regulated (14, 15). The large clusters formed by this mutant were refractive to *B. thuringiensis* swimmers. This limit to swimming activity suggests a threshold matrix density or the existence of specific matrix components that can obstruct penetration of swimmers. More experiments are required to make definitive assignments on the matrix factors that impede swimmers.

All together, these results show that motile bacilli can perturb heterologous biofilm populations, and highlight the importance of matrix properties for swimming capacity in a given swimmer-biofilm couple.

Swimmer Infiltration Sensitizes *S. aureus* Biofilms to Chemical Antimicrobials. These results showed that macromolecules gain entry into biofilms by means of tunnels formed by motile bacteria. We considered that this phenomenon would facilitate penetration, and hence effectiveness, of exogenously added disinfectants. This was tested using different bacillus species and benzalkonium chloride, a biocide frequently used in hospital and industrial settings, where biofilms are a common occurrence. *S. aureus* RN4220 biofilms were preexposed or not preexposed to *B. thuringiensis* 407 and *B. licheniformis* LMG 7560 swimmers, either separately or in combination, followed by a 5-min exposure to the disinfectant. Compared with the treatment in the absence of bacilli, which resulted in an eightfold decrease in *S. aureus* counts, swimmer-pretreated biofilms showed a decrease in counts of ~100-fold, with a synergistic effect (>300-fold decrease) in the presence of both motile strains (Table 1). The transient pores generated by motile bacteria can thus potentiate killing of biofilm bacteria by toxic substances in the environment.

Table 1. Swimmer infiltration sensitizes *S. aureus* biofilms to biocide killing

	No addition	Treatment with BAC*				
		No swimmers	*Bt* Δ*fla*	*Bt*	*Bl*	*Bl* + *Bt*
Log reduction (±0.2)	0	−0.9	−0.7	−1.7	−2.1	−2.5

S. aureus RN4220 24-h biofilms were submitted to a 4-h preincubation with bacillus swimmers *B. thuringiensis* 407 (*Bt*) or *B. licheniformis* LMG 7560 (*Bl*), or a mixture *Bl* + *Bt,* or with the nonmotile *Bt*Δ*fla* mutant. Biofilms were then disinfected with BAC. Standard errors were calculated from at least 16 values for each condition obtained in five independent experiments. The log reduction corresponds to the nontreated-to-treated ratio of *S. aureus* biofilms.
*BAC was used at 750 ppm for 5 min. Conditions and *S. aureus* colony-forming unit determinations (log reduction) are provided in *Materials and Methods*.

***S. aureus* Biofilms Are Disrupted and Supplanted by *B. thuringiensis* Swimmers Expressing a Biocide.** Numerous nonpathogenic bacteria secrete bactericidal molecules that are likely produced to reduce microbial competition (e.g., hydrogen peroxide, bacteriocins, antibiotics, autolysins) (16, 17). We reasoned that microbial motility could create a channel for in situ delivery of self-produced active bactericides to disrupt and repopulate the biofilms. As proof of principle, the integrity of biofilms formed by *S. aureus* (strain RN4220 expressing GFP) was challenged using either of two motile bacillus species (*B. thuringiensis* 407 and *B. subtilis* 168) expressing the *S. aureus*-specific cell wall endopeptidase, lysostaphin (18, 19). Biofilms that were untreated or treated with nonmotile *B. thuringiensis* expressing lysostaphin (*Bt*Δ*fla*, Fig. 3) remained essentially intact, and their biovolumes were not statistically different (*P* > 0.05). Remarkably, motile *B. thuringiensis* producing lysostaphin eradicated *S. aureus* within 24 h (Fig. 3). Supernatants alone or mobile non–lysostaphin-producing cells had no visible effect in the tested conditions. Equivalent results were obtained when 48-h *S. aureus* biofilms were exposed to the *B. thuringiensis* lysostaphin-producing strain. Experiments using corresponding *B. subtilis* strains and the motility-minus Δ*hag* mutant expressing or not expressing lysostaphin gave results equivalent to those obtained with *B. thuringiensis* (Fig. S2). Moreover, similar results with lysostaphin-producing *B. thuringiensis* were obtained when tested against biofilms comprising other *S. aureus* isolates of different origins (ATCC strains 6538, 27217, and 29247). These results clearly demonstrate that motility gives toxin-carrying bacteria access deep into the biofilm layers to eradicate a preexisting population.

Counterstaining with the red nucleic acid dye SYTO 61 of the residual treated biofilms revealed a dense 3D spatial arrangement of cells visible on the surface. In our experimental conditions, *B. thuringiensis* 407 appear red (SYTO 61 colors all cells) and *S. aureus* RN4220 is GFP-tagged and appears as green or yellow (depending on relative intensities of GFP and SYTO 61). *B. thuringiensis* eradicates *S. aureus* and concomitantly builds up a new biofilm structure on the cleared surface. Eradication and replacement of the *S. aureus* biofilm were similarly observed when motile *B. subtilis* 168 was used as the bactericide carrier strain (Fig. S2).
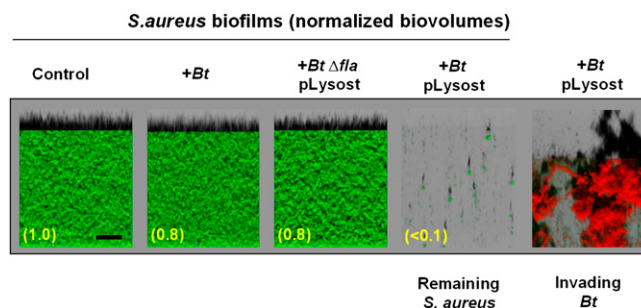

S.aureus biofilms (normalized biovolumes)

Control	+*Bt*	+*Bt* Δ*fla* pLysost	+*Bt* pLysost	+*Bt* pLysost
(1.0)	(0.8)	(0.8)	(<0.1)	
			Remaining *S. aureus*	Invading *Bt*

Fig. 3. Biocide-carrying motile *B. thuringiensis* eradicates and supplants *S. aureus* biofilms. Confocal observations of *S. aureus* RN4220 GFP biofilms after treatment with motile *B. thuringiensis* 407 (+*Bt*), motile *Bt* expressing lysostaphin (+*Bt* pLysost), and nonmotile cells expressing lysostaphin (+*Bt* Δ*fla* pLysost). In these experiments, *S. aureus* biofilms were 24 h old before being exposed to *Bt*. (Scale bar = 30 μm.) In the lower left-hand corner of each confocal image is the quantification of the residual biovolume (μm³) of *S. aureus* GFP biofilms after contact with *B. thuringiensis*; each value is the average of ~18 measurements performed in at least nine independent wells.

www.manaraa.com

Discussion

Microbial cells in a biofilm are generally considered as sessile and entrapped within their EPS (1, 2). Discovery of high-speed swimming planktonic cells tunneling deep within the biofilm structure changes this widely accepted view of biofilm structure. Our results support a straightforward mechanism for biofilm tunneling, in which nonmutated swimmers from the general planktonic population penetrate the biofilm matrix. It is notable that several swimmer bacteria tested in these studies were initially isolated from medically or industrially related surfaces, supporting the pertinence of the reported phenomenon in nature. The physical and regulatory mechanisms that modulate stealth swimming within the biofilm matrix (e.g., to limit swimming in same-species biofilms) remain to be identified and are the subject of future studies.

The disturbances generated by tunnel formation have dual consequences: "Like" bacteria may be advantaged in that tunnels increase macromolecular transfer and may thereby improve nutrient availability and reduce harmful gradients (e.g., of pH, of secreted toxic end products). Conversely, swimming heterologous bacteria, particularly those expressing antimicrobial products, may gain a foothold in established biofilms to destroy and replace a preexisting population. In this way, bacterial swimmers may introduce rapid changes in the biofilm population.

Role of a Minor Bacterial Subpopulation in Biofilm Dynamics.
The massive effects of the minor swimmer population (estimated as 0.1–1%) on biofilm structure and composition are unexpected in view of previous work. First, global approaches on biofilms would not detect expression changes or the influence of such minor subpopulations. Second, in pioneering fluorescent imaging studies of *B. subtilis* biofilms, expression of flagella was detected and shown to persist as a minor subpopulation in biofilm bacteria (20). In the present study, *B. subtilis* swimmers in its same strain biofilm did not generate discernible perturbations, possibly explaining why this phenomenon went unnoticed.

The swimming phenomenon differs from the previously reported event of biofilm dispersal, in which motile cells differentiate within biofilm mushroom-like structures present in large clusters of mature biofilm communities. These cells spread, promoting active seeding and dispersal (10, 21). In contrast, stealth swimmers were observed in mature biofilms and also in early stages of biofilm formation (Fig. S1). Importantly, our results indicate that stealth swimmers originate from planktonic cells rather than from the biofilm itself. All together, these differences indicate that dispersal and stealth swimming are distinct events. We suggest that a persisting swimming subpopulation is a determinant of biofilm integrity, propagation, and turnover.

Dual Role of Motile Subpopulations in a "Biological Insurance" Hypothesis.
It was previously hypothesized that diversity is a form of biological insurance that can safeguard the community in face of adverse conditions (22). The coexistence of sessile and motile subpopulations is an example of self-generated diversity. According to current thinking, a gradually decreasing substrate availability with time leads to slow or no growth in the deeper layers of a biofilm (2). In accordance with the biological insurance model, we suggest that planktonic swimmers can increase nutrient availability and gas and solute exchanges within the bulk biofilm fluid, which would favor regrowth within the deep biofilm layers by surrounding or entering cells. Alternatively, in specific niches, the existence of a motile subpopulation may be part of the equilibrium of the established community (e.g., by favoring cooperation between the microorganisms of the different layers, via solute exchanges as suggested by our work). This advantage may be reversed, however, in adverse medium, because tunneling by swimmers can also increase contact between biofilm bacteria and biocides, which would lead to accelerated cell death.

Numerous flagellated microorganisms naturally produce antimicrobial peptides, lipopeptide antibiotics, or bacteriocins, suggesting that the demonstrated biofilm assault phenomenon may occur in nature. In the case of heterologous motile species expressing antimicrobials, not only do they kill the existing biofilm bacteria but they may take over and replace them. Our findings suggest that, depending on the context, stealth swimmers can either contribute to community well-being or accelerate its destruction.

Applications of Motility to Pathogenic Biofilm Elimination.
Biofilms in industry and medicine remain a principal source of contamination and infection (3, 4). Although physical disruption has been the mainstay for industrial elimination of biofilms, biological strategies using specific molecules with antimicrobial or biofilm disruptive properties provide promising alternatives for biofilm control (23–25). Our studies on *S. aureus* biofilms show that irrigation by bacillus swimmers provides a conduit for biocides and potentiates biofilm disruption. An immediate application of swimmer-induced channels is to facilitate access to currently used surface disinfectants, such as oxidizing agents or quaternary ammonium compounds. Compared with planktonic cells, bacteria embedded in biofilms are typically 10- to 1,000-fold more resistant to these products (4, 26). Improved biocide efficacy against staphylococci in the presence of bacilli opens the door to novel treatment strategies that make use of lower amounts of environmentally polluting disinfectants. We showed that swimmers can also be put to work for in situ delivery of self-produced active antimicrobial molecules to disrupt heterologous biofilms. This strategy could be applicable to the elimination of pathogens in skin, nasal, or digestive infections (e.g., by using a motile bacteriocin-producing probiotic among *B. licheniformis* isolates). Natural or recombinant bacilli, or combinations of bacilli that synthesize antimicrobials, may constitute potent biofilm-disrupting mixtures that uproot and replace resident biofilm bacteria.

Materials and Methods

Biological Materials. Strains and plasmids used in this study are presented in Table S1.

Detection of Tunneling Subpopulations in the *B. thuringiensis* Biofilm Matrix.
B. thuringiensis 407 pHT315-GFP biofilms were cultivated in BST FC81 flow cells at 30 °C (Biosurface Technologies Corporation). To initiate biofilm growth, flow chambers were inoculated with 2 mL of exponential phase cultures diluted to $OD_{600} = 0.01$. Bacteria were allowed to attach to the substratum for 1 h without flow. LB (Difco) was then pumped continuously through the flow cell channel at 27 mL/h using a Watson–Marlow 205S peristaltic pump (Watson–Marlow Ltd.). Individual cell movements inside 48-h biofilms were examined by time-lapse confocal microscopy (Leica SP2 AOBS confocal microscope at the MIMA2 microscopy platform). Cells expressing GFP were excited at 488 nm with an argon laser, and fluorescence emission was collected on a photomultiplier detector in the range of 500–600 nm using an oil-immersion objective with a magnification of 63× (n.a. = 1.4). Individual single-cell trajectories were drawn manually from image series.

Each time series was registered with a 1.6-s interval between sequential images over a maximum period of 3 min. Images in these series were collected in four different regions deep within the biofilm matrix, about 5 μm above the coverslip. Individual cell movements in 24-, 48-, and 72-h biofilms were quantified using MATLAB 7.1 software (MathWorks). Moving cells can travel in any direction through the biofilm structure. Because recordings were made in the horizontal plane of the biofilm, only cells with sufficiently long trajectories (movement recorded through at least 2 sequential images separated by 1.6 s) in a given horizontal plane could be analyzed. The first and last positions of a given moving cell were taken into account to determine its mean velocity.

Typical cell mean velocities were determined by averaging bacterial movement over four regions of the biofilms, for ~50 cells for each biofilm. To estimate the circular rotation frequency of cell chains, we selected cells with a dominant rotation in the observation plane. Rotation frequencies of cell chains were averaged, as were mean velocity determinations.

Houry et al.

MICROBIOLOGY

Evolution of Matrix Strength According to Biofilm Age. The degree of thermal oscillations of sessile *B. thuringiensis* 407 cells was used as a matrix compactness indicator. To compare cell oscillation frequency within biofilms of different ages, we assume that there is no preferred oscillation direction/plane that would differ according to biofilm age. The analytical approach used to estimate cell oscillation is based on the statistical fluctuations of the cells within the analyzed regions. Selected regions were devoid of detectable motile cells within the range of time recorded. We attribute short-time variations in fluorescence intensity (FI) to the fluctuations of the number of cells in the recorded area. Fluorescence periodicity in the area, interpreted as thermal oscillation of sessile cells, was determined from the derivative of fluorescence values with time. We averaged results from experiments corresponding to each biofilm age and normalized the frequency to 1 for 24-h biofilms.

Quantification of Planktonic Fluorescent Bacilli That Infiltrate the Biofilm Matrix. *Evaluation of the time necessary for pioneer planktonic cells to reach the bottom of biofilms.* Biofilms of *B. thuringiensis* 407 were grown in 96-well microscopic-grade microtiter plates (27). Bacterial suspensions were prepared as described above for flow biofilms. For each condition, a calibrated suspension (250 μL) was added in three wells and incubated at 37 °C. Nonadherent cells were removed after 1 h by rinsing wells and renewing culture medium with 250 μL of sterile trypticase soy broth (TSB, BioMérieux). After incubation at 37 °C for 24 h, the growth medium was replaced by calibrated suspensions (~10^8 cfu/mL) of *B. thuringiensis* 407-GFP. Individual movements of GFP-expressing cells deep within the biofilm (5 μm above the bottom of the biofilm) were recorded by time-lapse confocal microscopy 15 min after their deposition. *Visualization of matrix strength evolution according to biofilm age.* Twenty-four-hour and 72-h *B. thuringiensis* 407 biofilms grown in flow cells were perfused with 3 mL of an exponential phase culture of *B. thuringiensis* 407-GFP at a concentration of 10^8 cfu/mL The flow was stopped for 1 h. After this period, the flow was resumed at 15 mL/h, and after a 2-h incubation, fluorescent cells detected inside the biofilm were quantified by confocal microscopy and their biovolumes were estimated with the PHLIP MATLAB routine (27).

Analysis of the Exopolysaccharide Matrix Density. *B. thuringiensis* 407 biofilms grown for 24 h and 72 h in flow cells were perfused for 10 min with PBS to remove loosely attached material. After the flow was resumed, the biofilm was mechanically detached from the glass slides and suspended in 1 mL of PBS. The recovered suspension was dissociated in a Potter glass homogenizer operated with 10 pestle strokes at 4 °C. The suspensions were then centrifuged at 2,700 × *g* for 10 min at 4 °C, and the exopolysaccharide matrix was recovered from the supernatant and frozen until use. Sugar concentration (μg/mL) was determined using the phenol–sulfuric acid assay (28). Sugar density within the biofilms was calculated by dividing the measured sugar concentrations by the total biovolume (μm³) of cells initially present on the flow cell glass surface.

Kinetics of FITC–Dextran Penetration in *B. thuringiensis* Biofilms. Three biofilms of *B. thuringiensis* 407 (*Bt* WT) and Δ*motA* (*Bt* Δ*motA*) were grown in 96-well microscopic grade microtiter plates as described previously. For each of the six biofilms, 2D time-lapse confocal acquisition was started just before addition of 50 μL of fluorescent tracer in each well (FITC–dextran, 250 kDa per 1 mg/mL; Sigma). Fluorescence acquisition was performed every second for 10 min through an objective with a magnification of 10× (excitation of the fluorophore at 488 nm and fluorescence acquisition in the range of 500–600 nm). The increase of FI over time was extracted from image sequences and regressed with the exponential function FI = A.(1 − e$^{−kt}$), where A is the maximum fluorescence intensity (FI), k a rate constant, and A.k the initial slope of the curve, which reflects the initial kinetics of tracer penetration in the biofilm matrix.

Growth of Bacterial Biofilms in Microplates. *S. aureus*, *E. faecalis*, *L. monocytogenes*, *Y. enterocolitica*, and *P. aeruginosa* 24-h biofilms were prepared in microplates at 37 °C and in TSB as described above for *B. thuringiensis* 407 (strains are listed in Table S1). Disruption of *S. aureus* biofilms by biocides

was tested using the fluorescent strain RN4220 pALC2084 expressing GFP (29). The resulting biofilms had a thickness of around 30 μm. For some studies, 48-h rather than 24-h *S. aureus* biofilms were prepared for *B. thuringiensis* treatments.

***S. aureus* Biofilm Disruption by Chemical Biocides.** Two bacillus swimmer strains were used alone or in combination to irrigate *S. aureus* RN4220 GFP biofilms: *B. thuringiensis* 407 and strain LMG 7560 of *B. licheniformis*, a species used as a probiotic. As a negative control, biofilms were treated with the nonmotile *B. thuringiensis* 407 isogenic Δ*fla* mutant. Two hundred fifty microliters of overnight cultures at ~10^8 cfu/mL of *B. thuringiensis* 407, *B. thuringiensis* Δ*fla*, *B. licheniformis* LMG 7560, or a *B. thuringiensis* 407 *B. licheniformis* LMG 7560 mixture in equal concentrations was added to 24-h *S. aureus* RN4220 biofilms after supernatant removal. Microplates were incubated for 4 h at 37 °C to allow swimmer infiltration, and supernatants were removed just before disinfectant testing.

Biofilms sensitized or not sensitized by swimmers were treated with benzalkonium chloride C14 (BAC; Fluka), a biocide frequently used in food and medical environments. Two hundred microliters of BAC at 750 ppm (disinfected biofilms; note that BAC concentration approximates the industrially used concentration) or 200 μL of NaCl at 150 mM (untreated biofilm) was added in the wells. After 5 min of contact at 20 °C, 200 μL of a quenching solution (3 g/L L-α-phosphatidylcholine, 30 g/L Tween 80, 5 g/L sodium thiosulfate, 1 g/L L-histidine, 30 g/L saponin) was added in wells to neutralize biocide activity. Biofilms were then mechanically detached from slides and dispersed in 5 mL of the quenching solution. *S. aureus* survivors were enumerated on TSA agar after serial dilution in NaCl at 150 mM and incubation for 24 h at 37 °C. The log$_{10}$ reduction in pathogen colony-forming units was calculated by comparing the ratio of survivors of the disinfected biofilms with the untreated biofilm population.

Genetic Construction of *B. thuringiensis* 407 Strains Producing Lysostaphin. The gene encoding lysostaphin was PCR-amplified from plasmid pWG200 (18) by tailing with 5′ XhoI and 3′ XbaI restriction sites. The *aphA3* promoter (P$_{apha-3}$) was PCR-amplified from plasmid pDG783 (30) by tailing with 5′ EcoRI and 3′ XhoI sites. Resulting fragments were digested by the corresponding restriction enzymes and ligated into EcoRI-XbaI–restricted plasmid pHT1618 (31). The resulting plasmid, pHT50, carrying the P$_{aphA-3}$-driven lysostaphin gene was established using tetracycline selection in *B. thuringiensis* 407 and the isogenic Δ*fla* mutant (13, 32).

***S. aureus* Biofilm Disruption and Displacement by Motile Bacilli Expressing Lysostaphin.** Growth medium of 24-h *S. aureus* RN4220 biofilms was replaced by calibrated suspensions (~5 × 10^6 cfu/mL) of *B. thuringiensis* strains 407, 407 pHT50, or 407 Δ*fla* pHT50 by means of sterile growth medium. The microplate was then incubated for 1 h at 37 °C, after which the biofilm supernatant was replaced by fresh sterile LB. After a 24-h incubation at 37 °C, the residual *S. aureus* green fluorescent biofilms were analyzed using confocal microscopy. Quantification of the residual *S. aureus* biofilms was performed by image analysis with the PHLIP MATLAB routine, and 3D projections were built from z-image series with the Imaris 3D function (Bitplane).

Implantation of motile bacilli in place of the destroyed staphylococcal biofilms was detected by counterstaining biofilms cells using the red nucleic acid dye SYTO 61 at 5 μM (Invitrogen). All cells are stained red; *S. aureus* expressing GFP is colored green or yellow, whereas bacilli are red.

1. Flemming HC, Wingender J (2010) The biofilm matrix. *Nat Rev Microbiol* 8:623–633.
2. Stewart PS, Franklin MJ (2008) Physiological heterogeneity in biofilms. *Nat Rev Microbiol* 6:199–210.
3. Epstein AK, Pokroy B, Seminara A, Aizenberg J (2011) Bacterial biofilm shows persistent resistance to liquid wetting and gas penetration. *Proc Natl Acad Sci USA* 108: 995–1000.
4. Mah TF, O'Toole GA (2001) Mechanisms of biofilm resistance to antimicrobial agents. *Trends Microbiol* 9:34–39.
5. Litchman E (2010) Invisible invaders: Non-pathogenic invasive microbes in aquatic and terrestrial ecosystems. *Ecol Lett* 13:1560–1572.
6. Wintermute EH, Silver PA (2010) Dynamics in the mixed microbial concourse. *Genes Dev* 24:2603–2614.
7. West SA, Griffin AS, Gardner A, Diggle SP (2006) Social evolution theory for microorganisms. *Nat Rev Microbiol* 4:597–607.
8. Lemon KP, Higgins DE, Kolter R (2007) Flagellar motility is critical for *Listeria monocytogenes* biofilm formation. *J Bacteriol* 189:4418–4424.

www.manaraa.com

9. Tolker-Nielsen T, et al. (2000) Development and dynamics of *Pseudomonas* sp. biofilms. *J Bacteriol* 182:6482–6489.

10. McDougald D, Rice SA, Barraud N, Steinberg PD, Kjelleberg S (2012) Should we stay or should we go: Mechanisms and ecological consequences for biofilm dispersal. *Nat Rev Microbiol* 10:39–50.

11. Rogers SS, van der Walle C, Waigh TA (2008) Microrheology of bacterial biofilms in vitro: *Staphylococcus aureus* and *Pseudomonas aeruginosa*. *Langmuir* 24:13549–13555.

12. Klapper I, Rupp CJ, Cargo R, Purvedorj B, Stoodley P (2002) Viscoelastic fluid description of bacterial biofilm material properties. *Biotechnol Bioeng* 80:289–296.

13. Houry A, Briandet R, Aymerich S, Gohar M (2010) Involvement of motility and flagella in *Bacillus cereus* biofilm formation. *Microbiology* 156:1009–1018.

14. Hamon MA, Lazazzera BA (2001) The sporulation transcription factor Spo0A is required for biofilm development in *Bacillus subtilis*. *Mol Microbiol* 42:1199–1209.

15. Bridier A, et al. (2011) The spatial architecture of *Bacillus subtilis* biofilms deciphered using a surface-associated model and in situ imaging. *PLoS ONE* 6:e16177.

16. Abriouel H, Franz CM, Ben Omar N, Gálvez A (2011) Diversity and applications of Bacillus bacteriocins. *FEMS Microbiol Rev* 35:201–232.

17. Selva L, et al. (2009) Killing niche competitors by remote-control bacteriophage induction. *Proc Natl Acad Sci USA* 106:1234–1238.

18. Gaier W, Vogel RF, Hammes WP (1992) Cloning and expression of the lysostaphin gene in *Bacillus subtilis* and *Lactobacillus casei*. *Lett Appl Microbiol* 14:72–76.

19. Recsei PA, Gruss AD, Novick RP (1987) Cloning, sequence, and expression of the lysostaphin gene from *Staphylococcus simulans*. *Proc Natl Acad Sci USA* 84:1127–1131.

20. Vlamakis H, Aguilar C, Losick R, Kolter R (2008) Control of cell fate by the formation of an architecturally complex bacterial community. *Genes Dev* 22:945–953.

21. Marchal M, et al. (2011) Subinhibitory arsenite concentrations lead to population dispersal in *Thiomonas sp*. *PLoS ONE* 6:e23181.

22. Boles BR, Thoendel M, Singh PK (2004) Self-generated diversity produces "insurance effects" in biofilm communities. *Proc Natl Acad Sci USA* 101:16630–16635.

23. Ramage G, Culshaw S, Jones B, Williams C (2010) Are we any closer to beating the biofilm: Novel methods of biofilm control. *Curr Opin Infect Dis* 23:560–566.

24. Kolodkin-Gal I, et al. (2010) D-amino acids trigger biofilm disassembly. *Science* 328:627–629.

25. Romero D, Kolter R (2011) Will biofilm disassembly agents make it to market? *Trends Microbiol* 19:304–306.

26. Bridier A, Briandet R, Thomas V, Dubois-Brissonnet F (2011) Resistance of bacterial biofilms to disinfectants: A review. *Biofouling* 27:1017–1032.

27. Bridier A, Dubois-Brissonnet F, Boubetra A, Thomas V, Briandet R (2010) The biofilm architecture of sixty opportunistic pathogens deciphered using a high throughput CLSM method. *J Microbiol Methods* 82:64–70.

28. Dubois M, Gilles K, Hamilton J, Rebers P, Smith F (1956) Colorimetric method for determination of sugars and related substances. *Anal Chem* 28:350–356.

29. Malone CL, et al. (2009) Fluorescent reporters for *Staphylococcus aureus*. *J Microbiol Methods* 77:251–260.

30. Guérout-Fleury AM, Shazand K, Frandsen N, Stragier P (1995) Antibiotic-resistance cassettes for *Bacillus subtilis*. *Gene* 167:335–336.

31. Lereclus D, Vallade M, Chaufaux J, Arantes O, Rambaud S (1992) Expansion of insecticidal host range of *Bacillus thuringiensis* by in vivo genetic recombination. *Biotechnology (N Y)* 10:418–421.

32. Lereclus D, Arantès O, Chaufaux J, Lecadet M (1989) Transformation and expression of a cloned delta-endotoxin gene in *Bacillus thuringiensis*. *FEMS Microbiol Lett* 51:211–217.

33. Hamze K, et al. (2011) Single-cell analysis in situ in a *Bacillus subtilis* swarming community identifies distinct spatially separated subpopulations differentially expressing hag (flagellin), including specialized swarmers. *Microbiology* 157:2456–2469.

34. Daou N, et al. (2009) IlsA, a unique surface protein of *Bacillus cereus* required for iron acquisition from heme, hemoglobin and ferritin. *PLoS Pathog* 5:e1000675.

MICROBIOLOGY

Houry et al.